J Mater Sci: Mater Med (2008) 19:1661–1668
DOI 10.1007/s10856-007-3259-3

Sol–gel preparation and high-energy XRD study of $(CaO)_x(TiO_2)_{0.5-x}(P_2O_5)_{0.5}$ glasses (x = 0 and 0.25)

David M. Pickup · Kate M. Wetherall · Jonathan C. Knowles · Mark E. Smith · Robert J. Newport

Received: 11 April 2007 / Accepted: 13 August 2007 / Published online: 4 October 2007

Abstract Glasses from the $CaO–TiO_2–P_2O_5$ system have potential use in biomedical applications. Here a method for the sol–gel synthesis of the ternary glass $(CaO)_{0.25}(TiO_2)_{0.25}(P_2O_5)_{0.5}$ has been developed. The structures of the dried gel and heat-treated glass were studied using high-energy X-ray diffraction. The structure of the binary $(TiO_2)_{0.5}(P_2O_5)_{0.5}$ sol–gel was studied for comparison. The results reveal that the heat-treated $(CaO)_{0.25}(TiO_2)_{0.25}(P_2O_5)_{0.5}$ glass has a structure based on chains and rings of PO_4 tetrahedra, held together by a combination of electrostatic interaction with Ca^{2+} ions and by corner-sharing oxygen atoms with TiO_6 octahedra. In contrast, the $(TiO_2)_{0.5}(P_2O_5)_{0.5}$ glass has a structure based on isolated P_2O_7 units linked together by corner-sharing with TiO_6 groups. The results suggest that both the dried gels possess open porous structures. For the $(CaO)_{0.25}(TiO_2)_{0.25}(P_2O_5)_{0.5}$ sample there is a significant increase in Ca–O coordination number with heat treatment.

D. M. Pickup (✉) · K. M. Wetherall · R. J. Newport
School of Physical Sciences, University of Kent,
Canterbury CT2 7NH, UK
e-mail: dmp@kent.ac.uk

J. C. Knowles
Division of Biomaterials and Tissue Engineering,
UCL Eastman Dental Institute, 256 Gray's Inn Road,
London WC1X 8LD, UK

M. E. Smith
Department of Physics, University of Warwick,
Coventry CV4 7AL, UK

1 Introduction

Glasses of the general formula $CaO–TiO_2–P_2O_5$ have a variety of interesting properties which make them suitable for biomedical applications [1, 2] as bone cavity fillers, drug delivery systems, biodegradable reinforcing phase in the case of composites for bone fixation devices and tissue engineering scaffolds. Such materials can be prepared to be bioresorbable, with the release of Ca^{2+} ions stimulating cell proliferation. The TiO_2 content reduces the dissolution rate and allows this rate to be accurately controlled, and is likely to be of major importance for cellular activity as suggested by a number of studies of Ti metal and other Ti alloys, both in vitro and in vivo. In fact, a recent in vitro study of the behaviour of phosphate-based glasses has shown that addition of TiO_2 causes significant gene up-regulation [3]. It has also been shown that adding TiO_2 to bioactive calcium phosphate coatings improves the adhesion of the coatings to metallic substrates [4].

Preparing $CaO–TiO_2–P_2O_5$ glasses by sol–gel processing has some significant advantages with respect to melt-quenching methods. Firstly, glassy films can be prepared which allows scope for devices to be coated with a biocompatible layer, and secondly, the processing can be modified to produce porous materials which is important in tissue engineering where meso- and macrostructure are important in terms of cell growth and nutrient supply to regenerated tissue. The low temperature nature of the sol–gel route also offers potential for use in drug delivery devices, where the gel acts as a soluble matrix, and for the inclusion of biocompatible polymers in the synthesis to produce composite materials with improved mechanical properties. Although $TiO_2–P_2O_5$ glasses can readily be prepared by the sol–gel route [5, 6], to date there have been no reports of additions of CaO to sol–gel $TiO_2–P_2O_5$ glasses in the literature.

Here we report the first sol–gel preparation of a $(CaO)_{0.25}(TiO_2)_{0.25}(P_2O_5)_{0.5}$ glass. The structures of both the dried gel and the heat-treated glass have been characterised using high-energy X-ray diffraction (HEXRD). The structure of a $(TiO_2)_{0.5}(P_2O_5)_{0.5}$ sol–gel binary glass has also been studied to help understand the effect that the addition of CaO has on the structure.

2 Experimental procedures

2.1 Sol–gel preparation

The following reagents were purchased commercially and used without further purification: phosphorus pentoxide (P_2O_5, Aldrich, 99.99+%), ethanol (EtOH, Fluka, anhydrous) calcium methoxyethoxide (Ca-methoxyethoxide, ABCR, 20% in methoxyethanol), titanium isopropoxide ($Ti(OPr^i)_4$, Aldrich, >95%), 1:1 molar mixture of mono- and di-substituted n-butyl phosphate ($OP(OH)_2(OBu^n)$ and $OP(OH)(OBu^n)_2$, Alfa Aesar, ~98%), 2-methoxyethanol (MeO–EtOH, Aldrich, 99.8%), isopropanol (Pr^iOH, Aldrich, 99.5%), n-butanol (Bu^nOH, Aldrich, 99.8%) and hydrochloric acid (Fisher, 37 wt.%).

All reactions were carried out under dry conditions in a sealed vessel with magnetic stirring. The first step in the preparation of the $(CaO)_{0.25}(TiO_2)_{0.25}(P_2O_5)_{0.5}$ sol–gel was the synthesis of the phosphate precursor, a 1:1 molar mixture of mono- and di-substituted ethyl phosphate ($OP(OH)_2(OEt)$ and $OP(OH)(OEt)_2$). This was prepared by reacting P_2O_5 with dry ethanol as described elsewhere [7]. Liquid-state ^{31}P NMR (Jeol GSX 270 MHz) was used to check that the ethyl phosphate precursor had been successfully synthesized.

The sol–gel reaction itself consisted of first diluting $Ti(OPr^i)_4$ in 2-methoxyethanol at a molar ratio of 1:19. After allowing this mixture to cool (approximately ½ h), the Ca-methoxyethoxide was added dropwise. The metal precursors were allowed to react for 1 h before adding the ethyl phosphate using a syringe pump at a rate of 20 mL/h such that the molar ratio of metal (Ca or Ti) to ethyl phosphate was 1:4. Next the reaction mixture was cooled in an ice bath before adding a solution containing H_2O and HCl catalyst in isopropanol at a rate of 100 mL/h using a syringe pump. The molar ratio of H_2O:HCl:Pr^iOH used was 4:0.1:12 relative to the amount of $Ti(OPr^i)_4$. The resultant clear sol was poured into a polypropylene container and allowed to gel, which took around 12 h.

The preparation of the $(TiO_2)_{0.5}(P_2O_5)_{0.5}$ sol–gel followed a similar procedure except that the phosphorus precursor used was n-butyl phosphate. This was reacted with $Ti(OPr^i)_4$ in 2-methoxyethanol and gelation brought about by the fast addition of a H_2O/HCl/solvent mixture. The details of this procedure are given elsewhere [6].

Both samples were aged at room temperature for 7 days in sealed containers before drying at 60 °C for 3 weeks and at 120 °C for 24 h. The dried gels were heated to 350 °C to remove solvent, water and organic molecules. This calcination temperature was chosen on the basis of a thermogravimetric measurement from the $(CaO)_{0.25}(TiO_2)_{0.25}(P_2O_5)_{0.5}$ sample (carried out on a Netzsch STA409 PC thermal analyzer) which showed that the organic material remaining in the sample burns out at ~300 °C. More details of this result are given later. Characterisation necessary for analysis of the X-ray diffraction data was performed: elemental analysis (ICP-AES and gravimetric) was carried out by a commercial company (Medac Ltd) and macroscopic densities were determined by helium pycnometry using a Quantachrome Multipycnometer. The results of this characterisation are given in Table 1.

2.2 High-energy X-ray diffraction measurements

The HEXRD data were collected on Station 9.1 at the SRS. The finely powdered samples were enclosed inside a 0.5 mm thick circular metal annulus by kapton windows and mounted onto a flat-plate instrumental set-up. The wavelength was set at $\lambda = 0.4858$ Å, and calibrated using the K-edge of an Ag foil; this value was low enough to provide data to a high value of momentum transfer ($Q_{max} = 4\pi\sin\theta/\lambda \sim 23$ Å^{-1}). The data were reduced using a suite of programs written in-house: the initial stage of analysis of XRD data from an amorphous material involves the removal of background scattering, normalization, correction for absorption and subtraction of the self-scattering term [8]. No correction was made to account for multiple scattering since it may be neglected in high energy X-ray diffraction from thin samples such as these given the relatively low sample attenuation. The resultant scattered intensity, $i(Q)$, can reveal structural information by Fourier transformation to obtain the pair-distribution function:

$$T(r) = T^0(r) + \int_0^\infty Qi(Q)M(Q)\sin(Qr)\,d(Q) \qquad (1)$$

where $T^0(r) = 2\pi^2 r\rho_0$ (r is the atomic separation between atoms and ρ_0 is the macroscopic number density) and $M(Q)$ is a window function necessitated by the finite maximum experimentally attainable value of Q.

Structural information can be obtained from the diffraction data by modelling the Q-space data and converting the results to r-space by Fourier transformation to allow

Table 1 Sample characterisation of $CaO–TiO_2–P_2O_5$ sol–gel materials

Nominal composition	Heat treatment/°C	Measured composition/at.%						Density/gcm^{-3}
		P	Ca	Ti	O	C	H	
$(CaO)_{0.25}(TiO_2)_{0.25}(P_2O_5)_{0.5}$	125	6.2	1.8	1.8	26.8	17.2	46.1	1.54
	350	12.1	3.6	3.6	51.8	7.3	21.5	2.21
$(TiO_2)_{0.5}(P_2O_5)_{0.5}$	125	3.5	0	2.0	18.2	21.8	54.5	1.35
	350	11.4	0	6.7	52.9	7.4	21.6	1.96

comparison with the experimentally determined correlation function [9]. The Q-space simulation is generated using the following equation:

$$p(Q)_{ij} = \frac{N_{ij} w_{ij}}{c_j} \frac{\sin QR_{ij}}{QR_{ij}} \exp\left[\frac{-Q^2\sigma_{ij}^2}{2}\right] \quad (2)$$

where $p(Q)_{ij}$ is the pair function in reciprocal space, N_{ij}, R_{ij} and σ_{ij} are the coordination number, atomic separation and disorder parameter, respectively, of atom i with respect to j, c_j is the concentration of atom j and w_{ij} is the weighting factor. The weighting factors are given by:

$$w_{ij} = \frac{2c_i c_j f(Q)_i f(Q)_j}{\overline{f(Q)}^2} \qquad \text{if } i \neq j \quad (3)$$

or,

$$w_{ij} = \frac{c_i^2 f(Q)_i^2}{\overline{f(Q)}^2} \qquad \text{if } i = j \quad (4)$$

where $f(Q)$ represents the Q-dependant X-ray form factors.

The errors associated with the HEXRD data arise mainly from the fitting process due to the problem of overlapping correlation shells. They have been estimated on the basis of the tolerance that a particular parameter may have without significantly changing the overall quality-of-fit. Some additional systematic error may occur from the data reduction process as a result of the approximations subsumed into the various data corrections (e.g. for Compton scattering), but past analysis of test-sample data, and data collected at different wavelengths, suggest that these errors are small compared to those arising from the numerical modelling of the experimental data.

3 Results and discussion

3.1 Thermal analysis

Figure 1 shows the combined TGA/DSC (thermogravimetric analysis/differential scanning calorimetry) trace obtained from the thermal analysis of the dried $(CaO)_{0.25}(TiO_2)_{0.25}(P_2O_5)_{0.5}$ sol–gel. The TGA trace exhibits three regions of significant mass loss: a gradual loss of ~3% in the range 30–200 °C, a sharp decrease in mass of ~25% in the range 200–300 °C, and finally a loss of ~4% at about 750 °C. The first mass loss can be attributed to the evaporation of water and any remaining solvent from the gel. This assignment is supported by a broad endothermic peak in the DSC trace which is consistent with the consumption of heat energy to drive off the solvent and H_2O. The second sharp mass loss is most likely due to the loss of hydroxyls and unreacted alkoxide groups as consolidation of the sol–gel network structure occurs. This mass loss corresponds to two peaks in the DSC trace centred around 312 °C. The first endothermic peak corresponds to the energy required to drive the increase in cross-linking in the network structure, whilst the second exothermic peak is representative of the energy given out as the organic fragments released by the structural rearrangement combust. The third and final region of mass loss corresponds to a sharp exothermic peak in the DSC trace at 758 °C. This exothermic peak is probably due to the energy released as the sol–gel glass crystallises and the associated mass loss caused by the loss of further –OH groups as this phase change occurs.

On the basis of the results described above, a calcination temperature of 350 °C was chosen for the $(CaO)_{0.25}(TiO_2)_{0.25}(P_2O_5)_{0.5}$ sol–gel because it lies beyond the

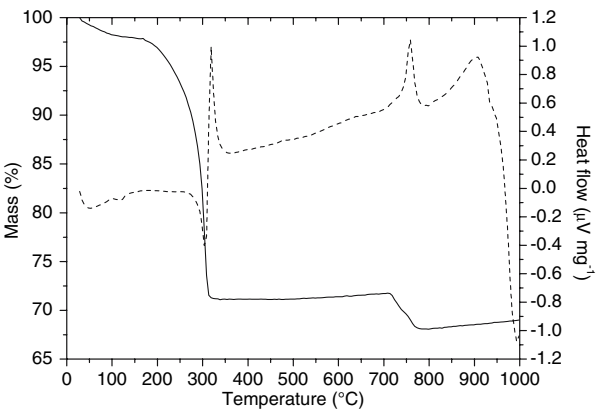

Fig. 1 Simultaneous TGA (solid line) and DSC (dashed line) measurements from the $(CaO)_{0.25}(TiO_2)_{0.25}(P_2O_5)_{0.5}$ sol–gel

temperature at which the organic fragments combust and yet well below the onset of crystallisation.

3.2 High-energy X-ray diffraction measurements

Figures 2–5 show the HEXRD data from the $(CaO)_{0.25}(TiO_2)_{0.25}(P_2O_5)_{0.5}$ and $(TiO_2)_{0.5}(P_2O_5)_{0.5}$ sol–gel samples, both prior to and after heat treatment. Both the *r*-space and *Q*-space data are shown, together with the fits to the pair-distribution functions obtained using the method described above. The structural parameters obtained from the fitting of the HEXRD data are given in Table 2.

It is well known that the building blocks of phosphate-based glasses are PO_4^{3-} tetrahedra [10, 11]. Each PO_4^{3-} can be connected to a maximum of three other such units to form a three-dimensional network, as in vitreous phosphorus pentoxide, *v*-P_2O_5. Metal oxides can be added to modify the network structure of the glass. Two P–O distances may be observed in phosphate glasses: a shorter distance of $\sim$1.5 Å ascribed to bonds to non-bridging oxygens (NBOs) and a longer distance of $\sim$1.6 Å due to bonds to bridging oxygens (BOs) [10–12]. The results in Table 2 from the $(CaO)_{0.25}(TiO_2)_{0.25}(P_2O_5)_{0.5}$ samples are consistent with the presence of two P–O distances at 1.50 and 1.58 Å which are respectively assigned to those due to bonds to non-

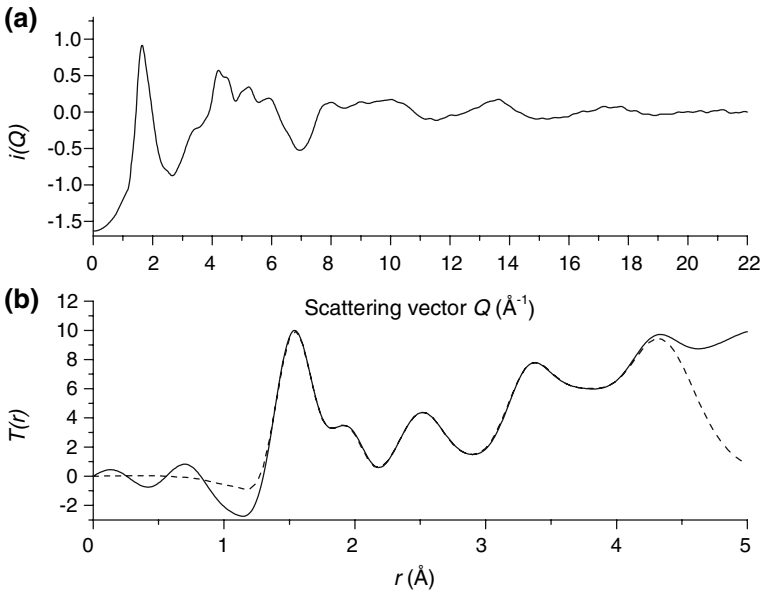

Fig. 2 X-ray diffraction data from the $(CaO)_{0.25}(TiO_2)_{0.25}(P_2O_5)_{0.5}$ sol–gel dried at 120 °C: (**a**) *Q*-space interference function, *i(Q)*, and (**b**) pair-distribution function, *T(r)*, (solid line) together with fit (dashed line)

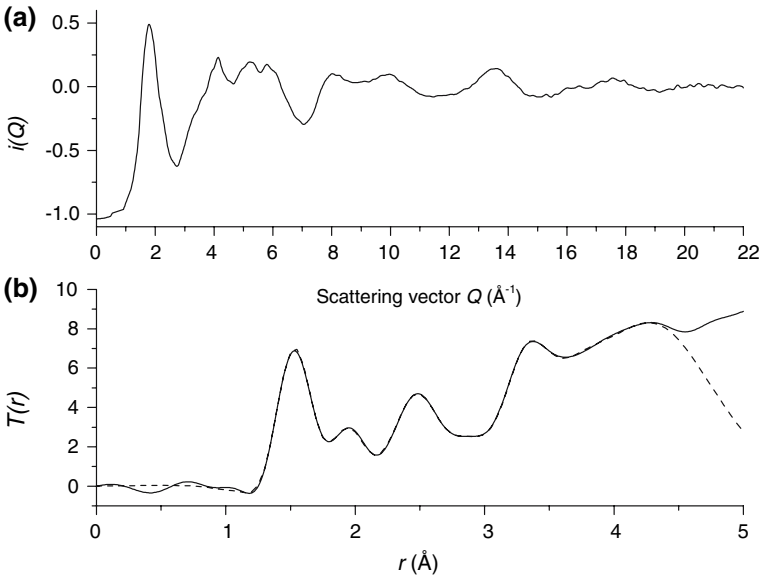

Fig. 3 X-ray diffraction data from the $(CaO)_{0.25}(TiO_2)_{0.25}(P_2O_5)_{0.5}$ sol–gel heat treated at 350 °C: (**a**) *Q*-space interference function, *i(Q)*, and (**b**) pair-distribution function, *T(r)*, (solid line) together with fit (dashed line)

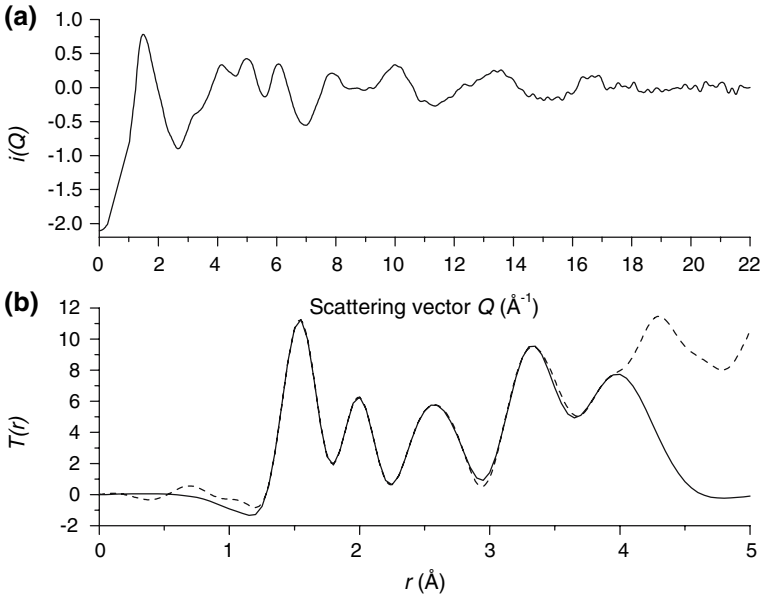

Fig. 4 X-ray diffraction data from the $(TiO_2)_{0.5}(P_2O_5)_{0.5}$ sol–gel dried at 120 °C: (**a**) *Q*-space interference function, *i(Q)*, and (**b**) pair-distribution function, *T(r)*, (solid line) together with fit (dashed line)

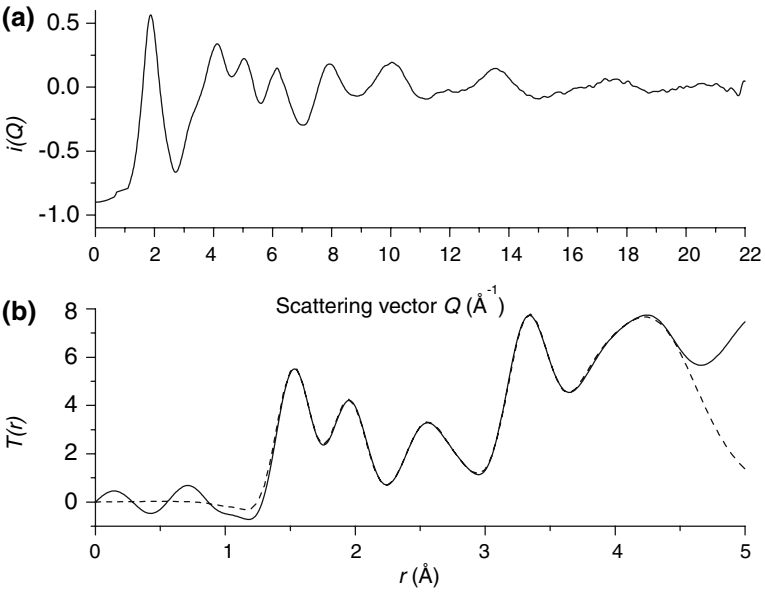

Fig. 5 X-ray diffraction data from the $(TiO_2)_{0.5}(P_2O_5)_{0.5}$ sol–gel heat treated at 350 °C: (**a**) *Q*-space interference function, *i(Q)*, and (**b**) pair-distribution function, *T(r)*, (solid line) together with fit (dashed line)

bridging and bridging oxygen atoms. For the sample heated to 350 °C, the total P–O coordination number is 4.5 which is in reasonable agreement with the expected value of 4 for PO_4^{3-} tetrahedra. Phosphate glasses at the metaphosphate composition, that is $(M_xO)_{0.5}(P_2O_5)_{0.5}$, are expected to have an equal number of P–NBO and P–BO bonds [10] so on average each phosphorus atom will be bonded to two bridging oxygens and two non-bridging oxygens. The P–NBO and P–BO coordination numbers for the $(CaO)_{0.25}(TiO_2)_{0.25}(P_2O_5)_{0.5}$ 350 °C sample are 2.4 and 2.1, respectively, and close to those expected for a glass at the metaphosphate composition. The fact that the number of NBOs is slightly higher than the number of BOs reflects the fact that the P/M atomic ratio is 1.7 (see Table 1) which is less than the value of 2 for the ideal metaphosphate composition. The higher metal oxide content results in reduced connectivity of the PO_4^{3-} network and, hence fewer BOs and correspondingly more NBOs. For the $(CaO)_{0.25}(TiO_2)_{0.25}(P_2O_5)_{0.5}$ sample dried at 120 °C, a total P–O coordination number of 5 is determined which is higher than expected for a phosphate-based material. This discrepancy is most likely due to the presence of organic material, such as unreacted alkoxide groups and occluded solvent. The C–C bond distance in an alkyl chain is 1.5 Å

Table 2 Structural parameters obtained from the fitting of the HEXRD data

Sample	Heat treatment/°C	Correlation	R/Å	N	σ/Å
$(CaO)_{0.25}(TiO_2)_{0.25}(P_2O_5)_{0.5}$	120	P–O	1.50(1)	2.0(2)	0.02(1)
		P–O	1.58(1)	3.0(2)	0.04(1)
		Ti–O	1.92(1)	5.9(2)	0.06(1)
		Ca–O	2.36(2)	2.1(4)	0.10(3)
		O–O	2.52(2)	3.1(3)	0.07(2)
		O–O	2.74(2)	2.5(5)	0.13(4)
		P–P	3.00(3)	1.0(4)	0.10(3)
$(CaO)_{0.25}(TiO_2)_{0.25}(P_2O_5)_{0.5}$	350	P–O	1.50(1)	2.4(2)	0.03(1)
		P–O	1.58(1)	2.1(2)	0.04(1)
		Ti–O	1.94(1)	5.9(2)	0.07(1)
		Ca–O	2.35(2)	4.4(4)	0.09(2)
		O–O	2.51(1)	3.9(3)	0.07(2)
		O–O	2.73(2)	2.2(5)	0.13(4)
		P–P	2.94(2)	2.1(4)	0.11(3)
$(TiO_2)_{0.5}(P_2O_5)_{0.5}$	120	P–O	1.52(1)	3.7(2)	0.05(1)
		P–O	1.58(1)	2.2(2)	0.04(1)
		Ti–O	1.98(1)	5.2(2)	0.05(1)
		O–O	2.51(1)	4.1(2)	0.09(2)
		O–O	2.73(2)	3.6(3)	0.08(2)
		P–P	3.00(3)	0.5(3)	0.10(4)
		P–Ti	3.31(2)	5.0(5)	0.16(3)
$(TiO_2)_{0.5}(P_2O_5)_{0.5}$	350	P–O	1.52(1)	2.9(1)	0.04(1)
		P–O	1.58(1)	0.8(2)	0.04(1)
		Ti–O	1.94(1)	4.4(2)	0.07(2)
		O–O	2.52(1)	2.4(2)	0.06(2)
		O–O	2.73(2)	3.0(4)	0.13(3)
		P–P	3.00(3)	0.8(3)	0.09(3)
		P–Ti	3.32(2)	3.3(3)	0.11(2)

and therefore we can expect a contribution to the first peak in the pair-distribution function from the organic groups. By not accounting for this, we have overestimated the peak area due to P–O bonding and obtained a value for the coordination number which is too high.

Of particular importance in calcium-containing biomaterials is the structural environment of the Ca^{2+} ions [13], which relates both to bioactivity and biocompatibility. Both the $(CaO)_{0.25}(TiO_2)_{0.25}(P_2O_5)_{0.5}$ samples studied exhibit a Ca–O nearest-neighbour distance of ~2.35 Å. This distance agrees well with those measured previously in CaO-containing metaphosphate glasses by HEXRD [10]. The interesting result in Table 2 is the change in Ca–O coordination number from ~2 to ~4.5 between the dried gel and the sample heated to 350 °C. This change suggests significant structural evolution with heat treatment. It is proposed that this evolution is due to the nature of the Ca^{2+} site changing from an environment similar to that in the sol–gel precursor, Ca-methoxyethoxide, [14] to one similar to that adopted by calcium in a fully-densified metaphosphate glass [10]. The environment of calcium in Ca-methoxyethoxide consists of two short Ca–O bonds to the two alkoxide groups with longer bonds to 2-methoxyethanol ligands allowing the calcium ions to attain their preferred coordination [14]. The longer Ca–O bonds are expected to lie over a range of distances and therefore will contribute a very diffuse peak in the pair-distribution function which cannot be simulated reliably. Ca^{2+} in metaphosphate glasses is usually coordinated to between 5 and 7 oxygen atoms at a distance of between 2.33 and 2.39 Å [10].

The results in Table 2 suggest that the Ti^{4+} ions are surrounded by ~6 oxygen atoms at a distance of 1.92–1.94 Å. Ti–O bond distances exhibit a strong correlation with coordination number: average Ti–O bond distances for 4-coordinated Ti^{4+} fall in the range 1.71–1.83 Å, whereas those for 5-coordinated Ti^{4+} range from 1.88–1.92 Å and those for 6-coordinated Ti^{4+} are in the range

1.92–2.04 Å [15]. The average Ti–O bond distance and coordination number measured here lend themselves to the conclusion that titanium occupies an octahedral site in these $(CaO)_{0.25}(TiO_2)_{0.25}(P_2O_5)_{0.5}$ samples.

The O–O distances measured give information on the PO_4, CaO_x, and TiO_6 polyhedra that comprise the structure. Taking an average P–O bond length of 1.54 Å and assuming a tetrahedral angle of 109°, the calculated average O–O distance for the PO_4 group is 2.51 Å which agrees well with the shorter measured O–O distance of 2.51–2.52 Å. Following a similar process for a TiO_6 octahedron with an average Ti–O bond length of 1.93 Å, we arrive at an O–O distance of 2.73 Å which agrees with the longer measured O–O distance. The O–O distance in the CaO_x polyhedra is expected to be significantly longer than those associated with the PO_4 and TiO_6 groups. Assuming octahedral coordination of calcium and a Ca–O distance of 2.35 Å, we arrive at an O–O distance of over 3.3 Å. In a ternary material such as $(CaO)_{0.25}(TiO_2)_{0.25}(P_2O_5)_{0.5}$ there are other overlapping correlations around this distance, e.g. the P–Ti nearest-neighbour distance [6], making it almost impossible to derive reliable empirical information on the O–Ca–O bond distance solely from HEXRD data.

Phosphate glass structures are also characterised by a P–P distance which occurs at 2.95 Å [11]. This correlation is important because it gives information on the connectivity of the PO_4^{3-} units that comprise the phosphate back-bone of the structure. Examining the pair-distribution functions in Figs. 2 and 3, it may clearly be observed that there is more intensity in the 2.9–3.0 Å region of the *T(r)* from the sample heated to 350 °C than in that from the dried gel. This result is echoed by the parameters in Table 2 which show an increase in the P–P coordination number from ~ 1 to ~ 2 upon heat treatment. This is further evidence of the evolution of the structure with heat treatment, with the connectivity of the PO_4^{3-} units increasing as alkoxide and hydroxyl groups are driven off. The P–P coordination of close to two for the heat-treated sample is in good agreement with that expected for a metaphosphate glass [10], which are generally considered to consist of phosphate chains and rings.

For comparison and to help understand the effect that the addition of CaO has on structure, HEXRD data was measured from a $(TiO_2)_{0.5}(P_2O_5)_{0.5}$ sol–gel sample. The structure of a sol–gel derived $(TiO_2)_{0.5}(P_2O_5)_{0.5}$ glass has been studied previously using neutron and X-ray diffraction [6]. The results of the previous work revealed that the structure of the heat-treated glass consists of corner-sharing TiO_6 octahedra and PO_4 tetrahedra, with the latter present as P_2O_7 groups connecting the TiO_6 octahedra. The structural parameters in Table 2, obtained by fitting the X-ray data from the $(TiO_2)_{0.5}(P_2O_5)_{0.5}$ sol–gel sample heat treated at 350 °C, are consistent with this model. The P–P coordination number is close to one and the ratio of P–NBO to P–BO bonds is around three, both suggesting the presence of $P_2O_7^{4-}$ pyrophosphate groups. Despite the fact that the simulated Ti–O coordination number of 4.4 is slightly low, the Ti–O distance is nevertheless broadly consistent with the presence of TiO_6 octahedra. Finally, the P–Ti coordination number is close to three as expected for phosphate tetrahedra corner-sharing three of their oxygens with TiO_6 octahedra. Structural parameters for a $(TiO_2)_{0.5}(P_2O_5)_{0.5}$ sol–gel dried at 120 °C have not been previously reported. The parameters determined here suggest that the structure is similar to that of the heat-treated glass, consisting of corner-sharing PO_4 and TiO_6 polyhedra. The P–O, Ti–O and P–Ti distances are all as expected for this arrangement of atoms. Note that the total P–O coordination number is a little high, probably due to a contribution to the first peak in the pair-distribution function from the residual organic groups, as discussed previously. However, important differences are observed between the dried and heat-treated sol–gel. Firstly, the Ti–O distance is slightly longer in the dried gel, and secondly, the P–P coordination number is significantly lower. The former difference is probably a result of the difference in the textural properties. Examination of the literature reveals that hydrated titanium phosphates with open structures, such as the porous $Ti_2O(PO_4)_2(H_2O)_2$ [16] and the layered γ-$Ti(H_2PO_4)(PO_4)\cdot(H_2O)$ [17], have longer average Ti–O bond lengths, 1.98 and 2.00 Å respectively, than the non-hydrated, denser analogues, such as TiP_2O_7, which has an average Ti–O bond length of 1.92 Å [18]. Hence, the results here suggest that the dried $(TiO_2)_{0.5}(P_2O_5)_{0.5}$ sol–gel has a porous, open structure with water molecules and hydroxyls coordinating the Ti and P atoms to increase their coordination numbers to their preferred values. The latter difference in P–P coordination between the dried gel and heat-treated glass is also related to the open nature of the structure of the dried gel. As this sample is heated, water molecules and hydroxyl groups are driven off and more P–O–P bridges are formed, resulting in an increased P–P coordination number.

Finally, comparing the results from the $(CaO)_{0.25}(TiO_2)_{0.25}(P_2O_5)_{0.5}$ sample with those from the $(TiO_2)_{0.5}(P_2O_5)_{0.5}$ sample, it can be seen that the nature of the two structures are different. The former material has a structure based on chains and rings of PO_4 tetrahedra, held together by a combination of electrostatic interaction with Ca^{2+} ions and by corner-sharing oxygen atoms with TiO_6 octahedra, whereas the latter has a structure based on isolated P_2O_7 units linked together by corner-sharing with TiO_6 groups. However, both structures exhibit an increase in connectivity between the MO_x and PO_4 polyhedra that comprise them as a function of heat treatment.

4 Conclusions

The sol–gel preparation of $(CaO)_{0.25}(TiO_2)_{0.25}(P_2O_5)_{0.5}$ has been described, which to the best of our knowledge is the first report of such a synthesis. The results of a HEXRD study reveal that the structure of the heat-treated $(CaO)_{0.25}(TiO_2)_{0.25}(P_2O_5)_{0.5}$ sol–gel glass is based on chains and rings of PO_4 tetrahedra, held together by a combination of bonds between NBOs and Ca^{2+} ions, and by corner-sharing oxygen atoms with TiO_6 octahedra. This structure is significantly different from that of the related $(TiO_2)_{0.5}(P_2O_5)_{0.5}$ sol–gel glass which is comprised of isolated P_2O_7 units linked together by corner-sharing with TiO_6 groups. Significant structural changes occur during heat treatment in both samples. The dried gels possess open structures with very little P–O–P connectivity. Heat treatment increases the P–P coordination number in both samples via the loss of water molecules and hydroxyl groups. Heat treatment of the $(CaO)_{0.25}(TiO_2)_{0.25}(P_2O_5)_{0.5}$ sol–gel causes an increase in Ca–O coordination number as the Ca^{2+} environment evolves from similar to that in the sol–gel alkoxide precursor to one closer to that in a fully-densified metaphosphate glass.

Acknowledgements The authors wish to acknowledge funding from the EPSRC (EP/C000714, EP/C000633 and GR/T21080) and the use of the EPSRC Chemical Database Service at Daresbury. We thank Mark Roberts of the CCLRC Daresbury Laboratory for his assistance in the use of station 9.1.

References

1. M. NAVARRO, E. S. SANZANA, J. A. PLANELL, M. P. GINEBRA and P. A. TORRES, *Bioceramics* **17** (2005) 893
2. M. NAVARRO, M. P. GINEBRA and J. A. PLANELL, *J. Biomed. Res*. **67A** (2003) 1009
3. E. A. ABOU NEEL, M. BITAR, V. SALIH, M. ITO, T. MIZOGUCHI and J. C. KNOWLES, *Biomaterials*, doi:10.1016/j.biomaterials.207.03.018
4. L.-D. PIVETEAU, B. GASSER and L. SCHLAPBACH, *Biomaterials* **21** (2000) 2193
5. A. TANG, T. HASHIMOTO, H. NASU and K. KAMIYA, *Mater. Res. Bull.* **40** (2005) 55
6. D. M. PICKUP, R. J. SPEIGHT, J. C. KNOWLES, M. E. SMITH and R. J. NEWPORT, *Mater. Res. Bull.*, doi:10.1016/j.materresbull.2007.03.005
7. A. F. ALI, P. MUSTARELLI, E. QUARTERONE and A. MAGISTRIS, *J. Mater. Res.* **14**(2) (1999) 327
8. J. M. COLE, E. R. H. Van ECK, G. MOUNTJOY, R. ANDERSON, T. BRENNAN, G. BUSHNELL-WYE, R. J. NEWPORT and G. A. SAUNDERS, *J. Phys.: Condens. Matter* **13** (2001) 4105
9. P. H. GASKELL, in "Materials Science and Technology", edited by J. Zrzycky, Vol 9, (VCH, Weinheim, 1991) p. 175
10. R. K. BROW, *J. Non-Cryst. Solids* **263–264** (2000) 1
11. U. HOPPE, G. WALTER, R. KRANOLD and D. STACHEL, *J. Non-Cryst. Solids* **263–264** (2000) 29
12. A. C. HANNON, *Nucl. Instr. & Meth.* **A551** (2005) 88
13. L. J. SKIPPER, F. E. SOWREY, D. M. PICKUP, K. O. DRAKE, M. E. SMITH, P. SARAVANAPAVAN, L. L. HENCH and R. J. NEWPORT, *J. Mater. Chem.* **15** (2005) 2369
14. S. C. GOEL, M. A. MATCHETT, M. Y. CHIANG and W. E. BUHRO, *J. Am. Chem. Soc.* **113**(5) (1991) 1844
15. The United Kingdom Chemical Database Service, D. A. FLETCHER, R. F. MCMEEKING and D. PARKIN, *J. Chem. Inf. Comput. Sci*. **36** (1996) 746
16. D. M. POOJARY, A. I. BORTUN, L. N. BORTUN and A. CLEARFIELD, *J. Solid State Chem.* **132** (1997) 213
17. A. N. CHRISTENSEN, E. K. ANDERSON, I. G. ANDERSON, G. ALBRTI, M. NIELSEN and E. K. LEHMANN, *Acta Chem. Scand.* **44** (1990) 865
18. S. T. NORBERG, G. SVENSSON and J. ALBERTSSON, *Acta Crystallogr., Sect. C: Cryst. Struct. Commun.* **C57** (2001) 225